Supplementary Appendix

This appendix has been provided by the authors to give readers additional information about their work.

Supplement to: Awad MM, Katayama R, McTigue M, et al. Acquired resistance to crizotinib from a mutation in *CD74–ROS1*. N Engl J Med 2013;368:2395-401. DOI: 10.1056/NEJMoa1215530

SUPPLEMENTARY APPENDIX

TITLE

Acquired Resistance to Crizotinib From A Mutation in *CD74-ROS1*

TABLE OF CONTENTS

AUTHORS

Mark M. Awad, M.D., Ph.D., Ryohei Katayama, Ph.D., Michele McTigue, Ph.D., Wei Liu B.S., M.A., Ya-Li Deng B.S., Alexei Brooun, Ph.D., Luc Friboulet, Ph.D., Donghui Huang, Ph.D., Matthew D. Falk, B.S., Sergei Timofeevski, Ph.D., Keith D. Wilner, Ph.D., Elizabeth L. Lockerman, B.A., Tahsin M. Khan, B.A., Sidra Mahmood, B.A., Justin F. Gainor, M.D., Subba R. Digumarthy, M.D., James R. Stone, M.D., Ph.D., Mari Mino-Kenudson, M.D., James G. Christensen, Ph.D., A. John Iafrate, M.D., Ph.D., Jeffrey A. Engelman, M.D., Ph.D., and Alice T. Shaw, M.D., Ph.D.

SUPPLEMENTARY METHODS

Immunohistochemistry. Hematoxylin and eosin staining was performed on 5-µm sections from formalin-fixed paraffin-embedded (FFPE) tumor tissue.

ROS1 Fluorescence In Situ Hybridization (FISH). *ROS1* FISH was performed as previously described[1]. We used a break-apart FISH approach using BAC clones corresponding to the 5′ (RP11-835I21) and 3′ (RP11-1036C2) sequences flanking the *ROS1* gene labeled by nick translation in green and red, respectively. FFPE slides were deparaffinized, treated with protease, codenatured with FISH probes using a Hybrite slide processor (Abbott Molecular, Chicago, IL), washed, counterstained, cover-slipped, and analyzed using an Olympus BX61 fluorescence microscope (Olympus, Tokyo, Japan) equipped with red, green, and 4′,6-diamidino-2-phenylindole filters. Images were captured and analyzed using Cytovision software (Genetix, San Jose, CA). Positive cases were defined as tumors harboring more than 15% of cells with split signals.

RNA Isolation, RT-PCR, and Sequencing. Total RNA was isolated from pleural fluid, from a right lung core biopsy, and from autopsy specimens using the RNeasy mini kit (Qiagen, Valencia, CA) and reverse transcribed with the Superscript III cDNA synthesis kit with an oligo-dT primer (Life Technologies, Carlsbad, CA). PCR was performed using the following primers:

CD74 forward 5’-GGTCTTTGAGAGCTGGATGC-3’
ROS1 reverse 5’-CTTGCCAGAAGGGCAGTAAG-3’

The full length of the PCR amplicon was sequenced bidirectionally by Sanger dideoxynucleotide sequencing. Sequencing primers and PCR conditions are available upon request.

Isolation of genomic DNA for *ROS1* exon PCR. Genomic DNA was isolated from the patient’s tumors and normal liver tissue at autopsy with the DNeasy kit (Qiagen, Valencia, CA). *ROS1* exon 38 (which contains the coding sequence for amino acid position 2032) was amplified by PCR with the FastStart PCR Master kit (Roche Applied Science, Indianapolis, IN) with the following primers:

ROS1 exon 38 F 5’-CCAGGAGTTGGAAAACGAAG-3’
ROS1 exon 38 R 5’-TTAGCCCAGGGTTCTGATTG-3’

The PCR amplicon was sequenced bidirectionally by Sanger dideoxynucleotide sequencing with the same primers.

***ROS1* Deep Sequencing.** *ROS1* exons 34 to 42 (corresponding to the 3’ region of *ROS1* involved in the fusion to CD74) were PCR-amplified and barcoded from isolated genomic DNA with the Roche FastStart High Fidelity PCR system (Roche Applied Science, Indianapolis, IN). Primers for the PCR reactions s are as follows:

Exon 34 forward, 5'-GGCAACTTAGCTTTTATCTATG-3'
Exon 34 reverse, 5'-GGTATGATTAAGTAAACAGTTTGTT-3'
Exon 35 forward, 5'- AAAACACTTCAAATGCACTG-3'
Exon 35 reverse, 5'- GCAATGCGGAATTCATAG-3'
Exon 36 forward, 5'- GGGGAGACAAAAATGTTGCTATT-3'
Exon 36 reverse, 5'- GGTCAATCTTTGTAGATATGGTGAT-3'
Exon 37 forward, 5'- ATGTCTGCTATACTGATTCCTG-3'
Exon 37 reverse, 5'- AAGCGGACTTAAAACTTCTTAC-3'
Exon 38 forward, 5'- TTCTGTCATATCATCCAGCCTG-3'
Exon 38 reverse, 5'- GGCATTTGCATTATGAAACCAA-3'
Exon 39 forward, 5'- TCATGCAAACTAGATAACTACCTG-3'
Exon 39 reverse, 5'- CGTAATAACCCTGTATCCAGAA-3'
Exon 40-1 forward, 5'- TAGGGCTACTTCTTTGATTTC-3'
Exon 40-1 reverse, 5'- GAGTCCAAAGTCTCCAATCTT-3'
Exon 40-2 forward, 5'- AGACTATACCAGTCCACGGA-3'
Exon 40-2 reverse, 5'- GTTTGATGATTCTGTCAGCA-3'.
Exon 41 forward, 5'- TAAAGCAAACCCTCTACTATTC-3'
Exon 41 reverse, 5'- TTGGGGGATACATATGTTAAC-3'.
Exon 42 forward, 5'- GCTATTTACTTTCCCATCTTTC-3'
Exon 42 reverse, 5'- CTTTGTTCAGTTCACAGTGC-3'

For each exon, 10 ng of genomic DNA were used for PCR (including negative controls in which no DNA template was added). The amplification protocol consisted of a 2-minute incubation step at 95^{o}C, followed by 15 amplification cycles of 95^{o}C for 20 sec, 60^{o}C for 45 sec (decreasing by 0.5^{o}C each cycle), 72^{o}C for 30 sec, followed by another 25 amplification cycles of 95^{o}C for 20 sec, 53^{o}C for 45 sec, and 72^{o}C for 30 sec, and final step of extension at 72^{o}C for 10 minutes.

For amplicon library preparation, equal amounts of PCR product of each amplicon from the same sample were pooled, and 100 ng of each pooled sample was used for the Ion Plus Fragment Library Kit (Life Technologies, Carlsbad, CA) according to the manufacturer's protocol. In the library construction process, the 5′ ends of the forward primers were fused with the A-Adaptor plus Ion Xpress™ Barcode Adapters 1–16, and the reverse primers were fused with the P1-adapter (Life Technologies, Carlsbad, CA). Equimolar amounts of amplified barcoded library samples were pooled according to the concentration measured by Agilent 2100 Bioanalyzer (Agilent Technologies, Santa Clara CA). The emulsion PCR was carried out with 2.8 x 10^{8} DNA molecules from the pooled barcoded library applying Ion PGM™ Template OT2 200 Kit (Life Technologies, Carlsbad, CA), and later sequenced on an Ion 316TM chip (Life Technologies, Carlsbad, CA) with Ion PGM™ Sequencing 200 Kit v2 (Life Technologies, Carlsbad, CA). The barcode-specific sample data were analyzed by Life Technologies Torrent Suite version 3.4. Exported BAM files were reviewed using the Broad Institute's Integrative Genomics Viewer (IGV) version 2.2. In IGV, the "Coverage allele-freq threshold" was set to "0.01", and the "Shade mismatched bases by quality" was set to "0 to 20".

Sequencing with Ion AmpliSeq™ Comprehensive Cancer Panel. Genomic DNA (60 ng) from each patient sample was amplified using Ion AmpliSeq™ Comprehensive Cancer Panel (Life Technologies, Carlsbad, CA); barcoded sequencing libraries were constructed using Ion AmpliSeq™ Library Kit 2.0 and Ion Xpress™ Barcode Adapters 1–16 (Life Technologies, Carlsbad, CA). In each sequencing run, three amplified barcoded libraries were pooled in equimolar amounts to the concentration measured by Agilent 2100 Bioanalyzer (Agilent Technologies, Santa Clara CA). The emulsion PCR was carried out with 2.8 x 10^8 DNA molecules from the pooled barcoded library applying Ion PGM™ Template OT2 200 Kit (Life Technologies, Carlsbad, CA), and later sequenced on an Ion 318TM chip (Life Technologies, Carlsbad, CA) with Ion PGM™ Sequencing 200 Kit v2 (Life Technologies, Carlsbad, CA). The barcode-specific sample data was analyzed by Life Technologies Torrent Suite version 3.4. Mutations were called using Life Technologies Variant Caller version 3.4 and Ion Reporter version 1.4.

Expression Constructs. cDNAs encoding either wild type CD74-ROS1 (exon 6 of CD74 fused to exon 34 of ROS1), CD74-ROS1 with the G2032R mutation, or green fluorescence protein (negative control) were cloned into retroviral expression vectors as previously described[5].

Transfection of 293T Cells and Immunoblotting. Transient transfection of 293T cells with 3 μg of plasmid DNA was performed using the TransIT Transfection reagent (Mirus Bio, Madison, WI). Cells were split 12 hours after transfection and then 24 hours later, they were cultured with media containing various concentrations of drugs for 24 hours. Cells were resuspended in lysis buffer (20 mmol/L Tris, 150 mmol/L NaCl, 1% Nonidet P-40, 10% glycerol, 1 mmol/L EDTA, 1 mmol/L ethyleneglycoltetracetic acid, and protease and phosphatase inhibitors), incubated on ice for 10 minutes, and centrifuged for 5 minutes (15,000 rpm). Protein concentration determination and immunoblotting were performed as previously described[6]. The phospho-ROS1, ROS1, phospho-ALK (Y1604), and ALK antibodies were obtained from Cell Signaling Technology (Danvers, MA). The GAPDH antibody was obtained from Abcam (Cambridge, MA).

Amino Acid Sequence Alignment. ROS1 paralogs were identified using the Ensembl Genome Browser (www.ensembl.org). The kinase domain sequences used for sequence alignment were obtained from the Human Protein Reference Database (www.hprd.org), and sequences were aligned using the Protein Basic Local Alignment Search Tool (http://blast.ncbi.nlm.nih.gov).

Expression and purification of human ROS1 kinase domain. The sequence (MAHHHHHHDYGIPTTENLYFQGS) encoding 6XHis and a TEV (Tobacco Etch Virus) protease cleavage site was fused to the N-terminus of the human ROS1 kinase domain (residues 1934-2232) using PCR amplification and then cloned into pFastBac1 insect cell expression vector (Life Technologies, Carlsbad, CA). The G2032R mutation was generated using the Quik Change Site-Directed Mutagenesis Kit (Agilent Technologies, Santa Clara CA). A baculovirus stock was generated, Sf21 cells were infected, and cells were harvested 72 hours after infection. Frozen cell pellets were lysed with 1.5 volumes/weight of lysis buffer (50 mM Tris pH 8.0, 150 mM NaCl, 10% glycerol, and one Roche Complete Protease Inhibitor Cocktail Tablet [Roche Applied Science, Mannheim, Germany] per 50 ml of lysis buffer). Immobilized metal affinity chromatography (IMAC) purification was performed using a ProBond™ nickel-chelating resin (Life Technologies, Carlsbad, CA) according to the manufacturer's protocol. The protein was then dephosphorylated with purified histidine-tagged Lambda phosphatase and the histidine tag was cleaved by digestion at $4^{o}C$ overnight with TEV protease in lysis buffer supplemented with 20 mM imidazole. The digested protein was loaded back onto an IMAC column and flow through containing the cleaved ROS1 kinase domain was collected, concentrated, and loaded on Superdex 75 16/60 column pre-equilibrated with 25 mM Hepes pH 7.4, 150 mM NaCl, 5% glycerol, and 2 mM TCEP. Monomer peaks containing the ROS1 kinase were pooled together and subjected to *in vitro* autophosphorylation at room temperature in 25 mM Hepes pH 7.4, 150 mM NaCl, 5% glycerol, 2 mM TCEP, 20mM $MgCl_2$ and 5mM ATP. The autophosphorylation reaction was stopped with EDTA pH 8.0 (final concentration 100 mM) when the protein reached +3P, +4P state, as monitored by LCMS. EDTA was removed using a Superdex 75 16/60 column and fractions containing predominantly +3P protein were collected and concentrated to 12.2 mg/ml for crystallization.

Enzyme Kinase Assays. Inhibition of wild-type and G2032R ROS1 kinase activities was measured using a microfluidic mobility shift assay. The reactions were conducted in 50-µL volumes in 96-well plates, and contained 0.6 nM preactivated enzyme kinase domain, 3 µM peptide substrate (5'FAM-KKSRGDYMTMQIG-CONH2, CPC Scientific, Sunnyvale, CA), inhibitor (11-dose 3-fold serial dilutions, 2% DMSO final) or DMSO only, 1 mM DTT, 0.002% Tween-20, 0.1 µM sodium orthovanadate and 5 mM $MgCl_2$ in 25 mM Hepes, pH 7.1, and were initiated by addition of ATP at the K_m level following a 20-minute preincubation. The reactions were incubated for 1 hour at room temperature and stopped by the addition of 0.1 M EDTA, pH 8. The extent of reaction (~10% peptide substrate conversion with no inhibitor) was determined after electrophoretic separation of the fluorescently labeled peptide substrate and phosphorylated product on a LabChip EZ Reader II (Caliper Life Sciences, Hopkinton, MA). The apparent inhibition constants were calculated by fitting initial reaction rates to a version of the Morrison equation for tight-binding inhibitors using non-linear regression method (GraphPad Prism, GraphPad Software, San Diego, CA):

$$Vi = Vo\frac{[\mathbf{E}] - [\mathbf{I}] - \mathbf{Ki,app} + \sqrt{([\mathbf{E}] - [\mathbf{I}] - \mathbf{Ki,app})^2 + 4[\mathbf{E}]\mathbf{Ki,app}}}{2[\mathbf{E}]}$$

where *Vi* and *Vo* are initial reaction rates in the presence and absence of inhibitor, respectively, [E] is a total enzyme concentration, [I] is a total inhibitor concentration and Ki,app is the apparent inhibition constant. Before use, enzymes were activated by auto-phosphorylation by incubating 30 μM of protein with MgATP and confirming 3P-phospho-state by LCMS.

Crystal Structure. The structure of the related kinase ALK in complex with crizotinib (wwPDB ID = 2xp2) was used as the starting model for structure determination. Crystals were obtained by the hanging drop vapor diffusion method at 13˚C by mixing 1.5 μl of solution containing a 1:3 molar ratio of phosphorylated ROS1 kinase domain (12.2 mg/ml) to crizotinib and 1.5 μl of reservoir solution containing 25% (w/v) PEG 3350, 0.6 M potassium thiocyanate and 0.1 M sodium citrate tribasic dihydrate, pH5.6. Crystals were flash-frozen in liquid nitrogen after transfer to a 2-ul reservoir solution containing 25% (v/v) glycerol as a cryoprotectant. An X-ray data set (Rmerge = 0.058 for data in the range of 50-2.12Å) was collected on a Rayonix 300 detector at beamline 081D-1 at the Canadian Light Source synchrotron. Initial structure determination was done with the Molecular Replacment program Phaser[2] using the crystal structure of the ALK kinase domain in complex with crizotinib (PDB ID = 2xp2). The structure was refined with CNX 2005[3] and Coot[4]. The final 2.2Å structure has an R-factor of 0.2332 and an R-free of 0.2820. Residues not included in the model, due to poor electron density, include 1954-1956 of the P-loop and 2111-2122 of the Activation loop. The ROS1-crizotinib complex crystal structure has been deposited to the wwPDB with entry ID 3zbf.

Supplementary Figures

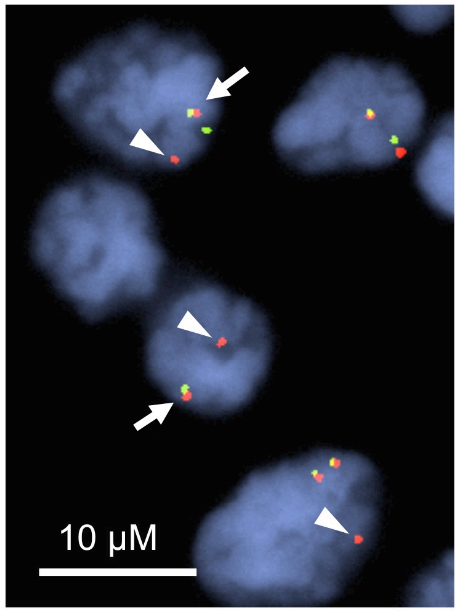

Figure S1. *ROS1* Fluorescence In Situ Hybridization of the Patient's Crizotinib-Resistant Tumor. Shown is a break-apart fluorescence in situ hybridization assay with a 5' *ROS1* probe (green) and a 3' *ROS1* probe (red) in the patient's formalin-fixed paraffin-embedded specimen. The *ROS1* rearrangement is detected by the presence of single isolated red 3' *ROS1* probes (arrowheads); no *ROS1* amplification was detected. The normal *ROS1* locus is shown as un-split red-green pair of probes (arrows). Nuclei are stained with 4',6-diamidino-2-phenylindole.

		RT-PCR and Sanger Sequencing	Targeted Sequencing ROS1 exons 34-42	AmpliSeq Comprehensive Cancer Panel			
Sample	**Estimated Tumor Cellularity**	**CD74-ROS1 Fusion**	**ROS1 G2032R**	**ROS1 G2032R**	**TP53 R175H**	**ATM Q201X**	**NOTCH2 S1068G**
Pre-treatment cells (early passage)	N/A	Detected	Not detected (27,031)	Not detected (408)	100% (114)	11% (1134)	75% (219)
Autopsy Site: Normal liver	0%	Not Detected	Not detected (24,972)	Not detected (221)	Not detected (74)	Not detected (170)	Not detected (319)
Autopsy Site: Chest wall tumor	30%	Detected	18% (27,678)	20% (103)	6% (141)	Not detected (214)	Not detected (171)
Autopsy Site: Right lung tumor #1	70% (+necrosis)	Detected	20% (30,147)	23% (243)	43% (102)	13% (466)	27% (164)
Autopsy Site: Right lung tumor #2	40% (+necrosis)	Detected	3% (14,798)	2% (179)	59% (78)	12% (85)	28% (18)
Autopsy Site: Mediastinal lymph node tumor	30% (+inflammation)	Detected	3% (15,996)	2% (186)	7% (174)	Not detected (250)	Not detected (241)
Autopsy Site: Left lung	5%	Detected	1.1% (11,939)	Not detected (464)	Not detected (74)	Not detected (545)	Not detected (197)

Figure S2. Deep Sequencing Analysis of Patient Samples. Patient samples and estimated percent tumor cellularity are listed. The red column highlights whether the *CD74-ROS1* fusion transcript was detected by RT-PCR and Sanger sequencing performed on RNA extracted from patient tissues. The blue column highlights the allele frequency (%) of the G2032R mutation as detected by targeted deep sequencing of *ROS1* exons 34-42. The yellow columns show the allele frequency (%) of somatic mutations detected in patient samples using the AmpliSeq Comprehensive Cancer Panel. To our knowledge, the ATM Q201X and NOTCH2 S1068G mutations have not been described previously. In each case, the number of sequencing reads is listed in parentheses below the allele frequency. There was insufficient genomic DNA from the original pre-treatment pleural effusion cell block for deep sequencing, so genomic DNA extracted from early-passage cultured pre-treatment cells was used for deep sequencing.

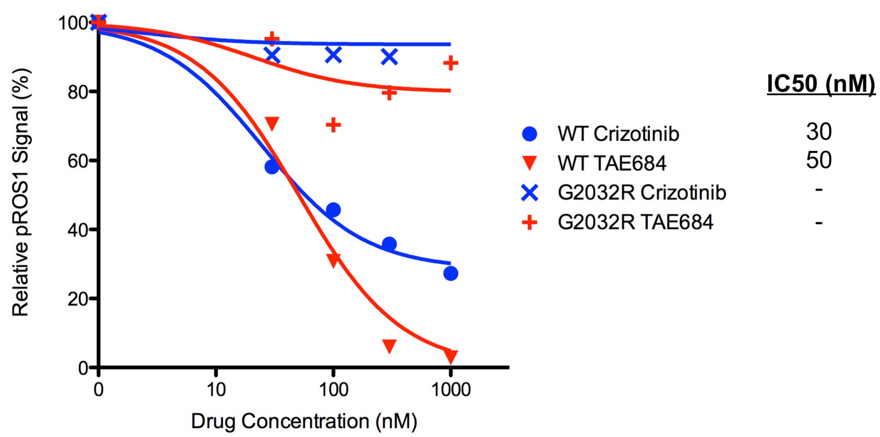

Figure S3. Estimation of IC50 Values for Inhibition of ROS1 Kinase Activity. Protein bands from the immunoblots shown in Figure 3B were quantified using Gene Snap software (Syngene). Phospho-ROS1 levels were normalized to total ROS1 levels. Dose response curves and IC50 values were determined using GraphPad Prism.

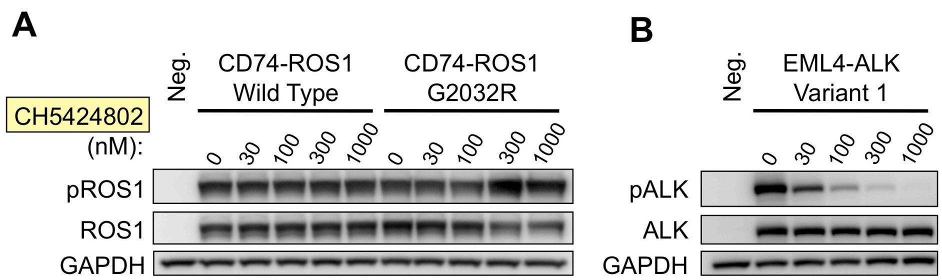

Figure S4. Lack of Activity of the ALK Inhibitor CH5424802 Against ROS1 Phosphorylation. 293T cells were transiently transfected with expression plasmids containing either wild-type *CD74-ROS1* or *CD74-ROS1* with the G2032R mutant. The transfected cells were treated with increasing concentrations of CH5424802 for 6 hours (Panel A). Lysates were prepared and western blot analyses were performed using the indicated antibodies. 293T cells were also transfected with a plasmid expressing green fluorescence protein as a negative (Neg) control. CH5424802 did not inhibit phosphorylation of either wild-type CD74-ROS1 or the G2032R mutant. As a positive control (Panel B), cells were transiently transfected with an *EML4-ALK* expression plasmid; increasing doses of CH5424802 led to effective inhibition of ALK phosphorylation.

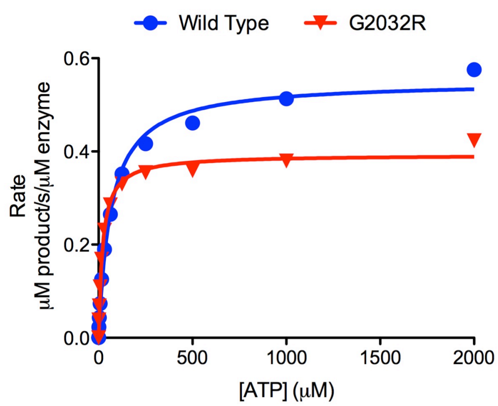

Figure S5. The ROS1 G2032R Mutant has a 3-Fold Lower K_m^{app} for ATP Compared to Wild Type. Shown are ATP-Km dependence of reaction rates for wild-type (K_m^{app} 65 µM) and G2032R (K_m^{app} 22 µM) ROS1 kinase domains. The initial reaction rates were measured by a mobility shift assay using 0.6 nM activated kinase domain enzymes, 3 uM 5'FAM-KKSRGDYMTMQIG-CONH2 and 0-2000 uM ATP as described in the Supplemental Methods section. The data were fit to the Michaelis-Menten equation to determine apparent ATP K_m values. Data points are mean values of duplicate measurements.

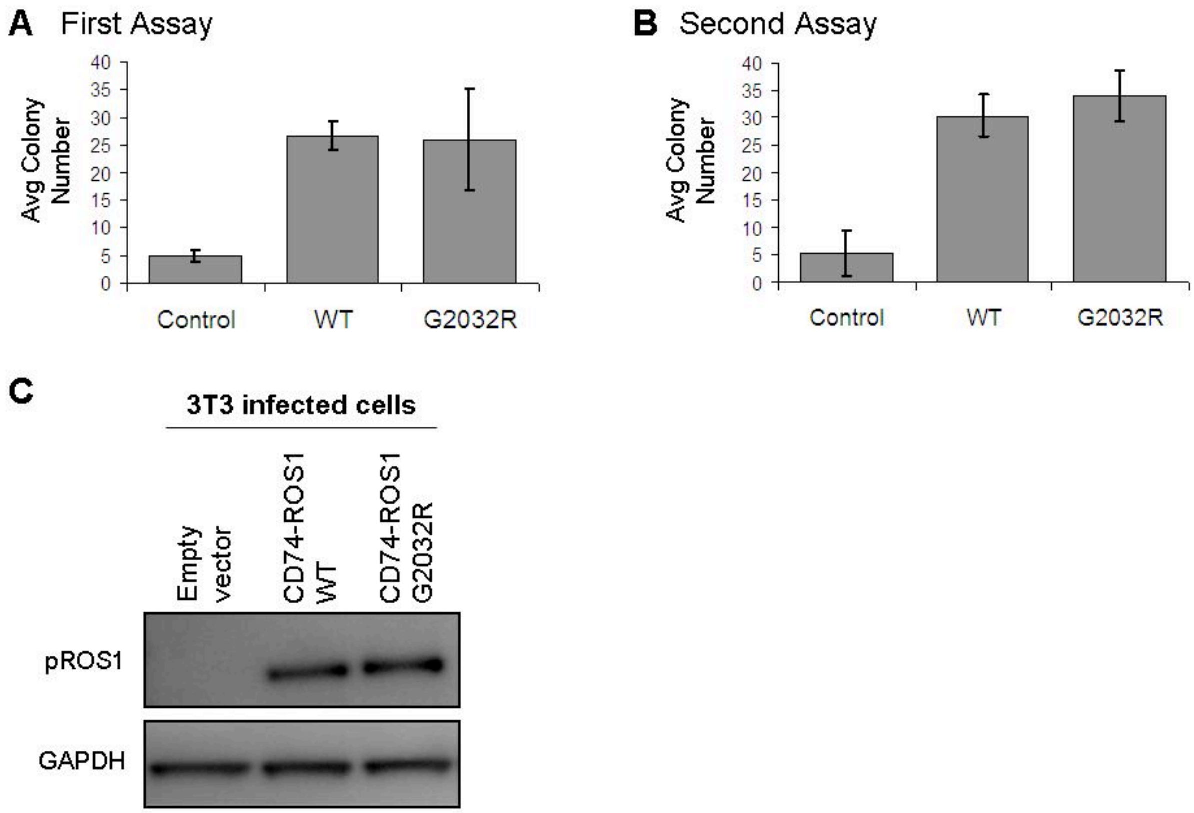

Figure S6. Soft Agar Assays to Evaluate Transforming Activity. Mouse 3T3 fibroblasts were infected with a lentivirus encoding *CD74-ROS1* or *CD74-ROS1* G2032R, followed by puromycin selection. Five thousand cells were mixed in 0.5% agarose and seeded on top of a layer of 1% agarose in 24-well plates. Numbers of transformed foci were counted manually in 2 independent experiments after either 20 days (Panel A) or 17 days (Panel B); standard deviation error bars are shown. Expression of CD74-ROS1 and mutant CD74-ROS1 was confirmed by immunoblotting for phospho-ROS1 (Panel C).

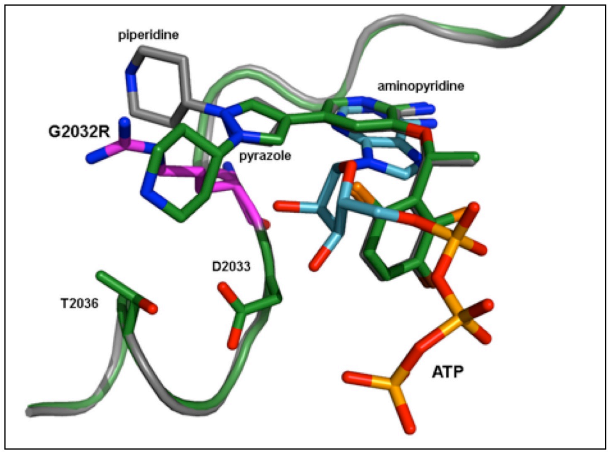

Figure S7. The Side Chain of R2032 is Predicted to Clash with the Crizotinib Piperidine Ring but Not with ATP. Superposition of the kinase hinge segment and crizotinib from the ROS1 complex (green) and the crystal structure of the ALK-crizotinib complex (grey, wwPDB ID = 2xp2). The position of ATP (carbon atoms shown in light blue) was modeled from the insulin receptor crystal structure (wwPDB ID=1ir3). A modeled position for the R2032 mutant side chain in uncomplexed ROS1 is shown in purple.

Figure S8. Amino Acid Sequence Alignment of the ROS and ALK Tyrosine Kinase Domains. Identical residues are highlighted in black and conserved substitutions are highlighted in gray. The G2032R *ROS1* mutation is shown in red above the aligned sequences, which corresponds to the G1202R *ALK* mutation (blue) found in crizotinib-resistant *ALK*-rearranged lung cancers. Other *ALK* mutations that have been found in crizotinib-resistant patients are shown in blue below the aligned sequences[7–9].

SUPPLEMENTARY REFERENCES

1. Bergethon K, Shaw AT, Ou S-HI, et al. ROS1 rearrangements define a unique molecular class of lung cancers. J Clin Oncol 2012;30(8):863–70.

2. McCoy AJ, Grosse-Kunstleve RW, Adams PD, Winn MD, Storoni LC, Read RJ. Phaser crystallographic software. J Appl Crystallogr 2007;40(Pt 4):658–74.

3. Brünger AT, Adams PD, Clore GM, et al. Crystallography & NMR system: A new software suite for macromolecular structure determination. Acta Crystallogr D Biol Crystallogr 1998;54(Pt 5):905–21.

4. Emsley P, Lohkamp B, Scott WG, Cowtan K. Features and development of Coot. Acta Crystallogr D Biol Crystallogr 2010;66(Pt 4):486–501.

5. Engelman JA, Zejnullahu K, Gale C-M, et al. PF00299804, an irreversible pan-ERBB inhibitor, is effective in lung cancer models with EGFR and ERBB2 mutations that are resistant to gefitinib. Cancer Res 2007;67(24):11924–32.

6. Engelman JA, Jänne PA, Mermel C, et al. ErbB-3 mediates phosphoinositide 3-kinase activity in gefitinib-sensitive non-small cell lung cancer cell lines. Proc Natl Acad Sci USA 2005;102(10):3788–93.

7. Choi YL, Soda M, Yamashita Y, et al. EML4-ALK mutations in lung cancer that confer resistance to ALK inhibitors. N Engl J Med 2010;363(18):1734–9.

8. Katayama R, Shaw AT, Khan TM, et al. Mechanisms of acquired crizotinib resistance in ALK-rearranged lung Cancers. Sci Transl Med 2012;4(120):120ra17.

9. Doebele RC, Pilling AB, Aisner DL, et al. Mechanisms of resistance to crizotinib in patients with ALK gene rearranged non-small cell lung cancer. Clin Cancer Res 2012;18(5):1472–82.